PREDICTION OF NONLINEAR AEROELASTIC INSTABILITIES

A. Sedaghat, J.E. Cooper, J. R. Wright and A.Y.T. Leung
Manchester School of Engineering
Manchester University, Manchester M13 9PL, UK

Abstract

This paper describes part of an investigation into the use of Normal Form Theory to predict and characterise Limit Cycle Oscillations (LCO) in non-linear aeroelastic systems. Starting with the coupled aeroelastic integro-differential equations of a system with non-linearities, it is shown how to reduce the order of the system and then compute the normal forms using a class of the period-averaging method. The stability of the LCO can then be characterised by considering the behaviour around the linear flutter condition. Such an approach does away with the need for numerical simulation of the system. The methodology is demonstrated upon a simple two-degrees-of-freedom aeroelastic wing model with cubic stiffness. A good agreement is obtained between analytical and simulation results.

1 Introduction

It is usual for the aeroelastic behaviour and flutter clearance to be made assuming linear aerodynamics and linear aircraft structure. However, the influence of non-linearities on modern aircraft is becoming increasingly important [1] and the requirement for more accurate predictive tools grows stronger. These non-linearities can be due to structural (free-play, backlash, cubic stiffness), aerodynamic (moving shocks and transonic effects) or control (time delays, control laws) phenomena.

Vibration behaviour such as Limit Cycle Oscillations (LCO) can only occur in non-linear systems [2,3]. Consequently, it is not possible to predict LCO using a purely linear analysis. Moreover, linear analysis is becoming less feasible. LCO has become an important research topic over the last few years, although such problems have been noted since the 1970s.

One area where there is an urgent need for a predictive capability is in envelope expansion during flight flutter tests. It is of particular interest to determine:

- whether an aircraft will experience Limit Cycle Oscillations and/or Flutter
- whereabouts in the flight envelope LCO phenomena will occur
- the precise nature of the LCO.

Although not desirable, LCO is essentially a fatigue problem, whereas flutter is usually catastrophic and must be avoided at all costs. An accurate LCO/flutter prediction capability would reduce significantly the amount of flights required in any flight clearance test programme with current costs being estimated at around $70k per test flight.

There has been much work in recent years [2-4] devoted towards the characterisation of non-linear aeroelastic behaviour, including LCO. This work has primarily consisted of simulating the response of the aeroelastic system through numerical integration, although there are a few known instances of experimental verification [5]. Some effort has employed techniques such as the Harmonic Balance method to address the problem. However, due to the assumptions made in modelling the non-linearity, the method does not produce accurate estimates of the LCO behaviour.

Much effort has been devoted [6,7] to improving unsteady CFD modelling allied to the coupling of the aerodynamic and structural grids. Significant headway has been made towards solving the problem, particularly in the Transonic region. However, there are still major problems inherent due to the enormous computational resources required for even the simplest cases. A number of mathematical techniques exist in the non-linear dynamics community that enables the stability boundaries of a defined non-linear system to be computed and the possible instabilities characterised. In this paper, Normal Form theory [8] has been implemented in such a way that it can be used on non-linear non-autonomous aeroelastic systems and to include the effects of unsteady aerodynamics. It should be noted that only cases where the non-linearities are continuous are considered.

Such an approach does away with the need for extensive computational simulations. However, the methodology is not seen as replacement for extensive CFD modelling, but as a guide to determine which parts of the flight envelope should be investigated using sophisticated CFD methods. This work is part of a research programme aimed at developing a complete modelling and predictive capability for non-linear aircraft.

The methodology of the proposed approach is described and then demonstrated upon a simple binary aeroelastic system with structural non-linearities. Comparison is made between the analytical and numerical integration results.

2 Governing Aeroelastic Equations

Consider a two-degree-of-freedom aerofoil oscillating in pitch and plunge as shown in Figure 1. The heave deflection is denoted by h, positive in the downward direction, α is the pitch angle about the elastic axis, positive with the nose up. The elastic axis is located at a distance $a_h b$ from the mid-chord while the mass centre is located at a distance $x_\alpha b$ from the elastic axis. Both distances are positive when measured towards the trailing edge of the aerofoil. The integro-differential aeroelastic equations of motion have been derived by Fung [9], and used here in non-dimensional form. The equations including structural non-linearities with incompressible fluid at speed U are written as

$$\begin{aligned}&\xi'' + x_\alpha \alpha'' + 2\zeta_\xi \frac{\bar{\omega}}{\bar{U}}\xi' + \left(\frac{\bar{\omega}}{\bar{U}}\right)^2 \xi + G(\xi) = -\frac{1}{\pi\mu} C_L(\tau) + \frac{P(\tau)}{mU^2}\\ &\frac{x_\alpha}{r_\alpha^2}\xi'' + \alpha'' + 2\zeta_\alpha \frac{1}{\bar{U}}\alpha' + \left(\frac{1}{\bar{U}}\right)^2 \alpha + M(\alpha) = \frac{2}{\pi\mu r_\alpha^2} C_M(\tau) + \frac{Q(\tau)}{mU^2 r_\alpha^2}\end{aligned} \tag{1}$$

where $\xi = h/b$ is the non-dimensional displacement and the prime superscript denotes differentiation with respect to the non-dimensional time τ which is defined as $\tau = U.t/b$. $\bar{U}$ is a non-dimensional velocity defined as $\bar{U} = U / b\omega_\alpha$, and $\bar{\omega}$ is given by $\bar{\omega} = \omega_\xi / \omega_\alpha$, where ω_ξ and ω_α are the uncoupled heaving and pitching modes natural frequencies, respectively. ζ_ξ and ζ_α are the damping ratios, r_α is the ratio of gyration about the elastic axis. $G(\xi)$ and $M(\alpha)$ are functions of the non-linear heave and pitch stiffness terms, respectively. $C_L(\tau)$ and $C_M(\tau)$ are the lift and pitching moment coefficients, respectively. For incompressible flow, the expressions for $C_L(\tau)$ and $C_M(\tau)$are [9]

$$\begin{aligned}C_L(\tau) &= \pi(\xi'' - a_h\alpha'' + \alpha') + 2\pi\phi(\tau)\left\{\alpha(0) + \xi'(0) + \left(\frac{1}{2} - a_h\right)\alpha'(0)\right\}\\ &+ 2\pi\int_0^\tau \phi(\tau-\sigma)\left(\alpha'(\sigma) + \xi''(\sigma) + \left(\frac{1}{2} - a_h\right)\alpha''(\sigma)\right)d\sigma\\ C_M(\tau) &= \frac{\pi}{2}a_h(\xi'' - a_h\alpha'') - \frac{\pi}{2}\left(\frac{1}{2} - a_h\right)\alpha' - \frac{\pi}{16}\alpha''\\ &+ \pi\left(\frac{1}{2} + a_h\right)\phi(\tau)\left\{\alpha(0) + \xi'(0) + \left(\frac{1}{2} - a_h\right)\alpha'(0)\right\}\\ &+ \pi\left(\frac{1}{2} + a_h\right)\int_0^\tau \phi(\tau-\sigma)\left(\alpha'(\sigma) + \xi''(\sigma) + \left(\frac{1}{2} - a_h\right)\alpha''(\sigma)\right)d\sigma\end{aligned} \tag{2}$$

where the Wagner function $\phi(\tau)$ is given by

$$\phi(\tau) = 1 - \psi_1 Exp(-\varepsilon_1\tau) - \psi_2 Exp(-\varepsilon_1\tau) \tag{3}$$

with constants $\psi_1=0.165$, $\psi_2=0.335$, $\varepsilon_1=0.0455$, and $\varepsilon_2=0.3$. $P(\tau)$ and $Q(\tau)$ are the externally applied forces and moments, respectively.

Having applied the Wagner function, the integro-differential equation (1) can be rewritten in a general form containing only differential operators using the following transformation

$$\begin{aligned} w_1 &= \int_0^\tau Exp(-\varepsilon_1(\tau-\sigma))\alpha(\sigma)d\sigma \\ w_2 &= \int_0^\tau Exp(-\varepsilon_2(\tau-\sigma))\alpha(\sigma)d\sigma \\ w_3 &= \int_0^\tau Exp(-\varepsilon_1(\tau-\sigma))\xi(\sigma)d\sigma \\ w_4 &= \int_0^\tau Exp(-\varepsilon_2(\tau-\sigma))\xi(\sigma)d\sigma \end{aligned} \tag{4}$$

from which the system (1) can be rewritten as

$$\begin{aligned} &c_0\xi'' + c_1\alpha'' + c_2\xi' + c_3\alpha' + c_4\xi + c_5\alpha + c_6 w_1 + \\ &c_7 w_2 + c_8 w_3 + c_9 w_4 + \left(\frac{\varpi}{U}\right)^2 \xi + G(\xi) = f(\tau) \\ &d_0\xi'' + d_1\alpha'' + d_2\alpha' + d_3\alpha + d_4\xi' + d_5\xi + d_6 w_1 + \\ &d_7 w_2 + d_8 w_3 + d_9 w_4 + \left(\frac{1}{U}\right)^2 \alpha + M(\alpha) = g(\tau) \end{aligned} \tag{5}$$

The coefficients c_0, c_1, …,c_9,d_1,…, $d9$ are given in the appendix A. $f(\tau)$ and $g(\tau)$ are functions depending on initial conditions, Wagner function and the external forces, and are given by

$$\begin{aligned} f(\tau) &= \frac{2}{\mu}\left(\left(\frac{1}{2}-a_h\right)\alpha(0)+\xi(0)\right)\begin{pmatrix}\psi_1\varepsilon_1 Exp[-\varepsilon_1\tau]+ \\ \psi_2\varepsilon_2 Exp[-\varepsilon_2\tau]\end{pmatrix} \\ &+\frac{P(\tau)b}{mU^2} \\ g(\tau) &= -\frac{(1+2a_h)}{2r_\alpha^2}f(\tau)+\frac{Q(\tau)}{mU^2r_\alpha^2} \end{aligned} \tag{6}$$

By introducing a variable vector $X=(x_1,x_2,\ldots,x_8)^T$ defined as

$$\begin{aligned} &x_1=\alpha, \quad x_2=\alpha', \quad x_3=\xi, \quad x_4=\xi' \\ &x_5=w_1, \quad x_6=w_2, \quad x_7=w_3, \quad x_8=w_4 \end{aligned} \tag{7}$$

The coupled equations given in (5) can now be written as a set of eight first order ordinary differential equations $X'=f(X,\tau)$ such that

$$\begin{cases} x_1' = x_2 \\ x_2' = (c_0H-d_0P)/(d_0c_1-c_0d_1) \\ x_3' = x_4 \\ x_4' = (-c_1H+d_1P)/(d_0c_1-c_0d_1) \\ x_5' = x_1-\varepsilon_1 x_5 \\ x_6' = x_1-\varepsilon_2 x_6 \\ x_7' = x_3-\varepsilon_1 x_7 \\ x_8' = x_3-\varepsilon_2 x_8 \end{cases} \tag{8}$$

where

$$\begin{aligned} P &= c_2x_4+c_3x_2+c_4x_3+c_5x_1+c_6x_5+c_7x_6+ \\ &\quad c_8x_7+c_9x_8+G(x_3)-f(\tau) \\ H &= d_2x_2+d_3x_1+d_4x_4+d_5x_3+d_6x_5+d_7x_6+ \\ &\quad d_8x_7+d_9x_8+M(x_1)-g(\tau) \end{aligned} \tag{9}$$

Equation (8) can be integrated numerically using Runge-Kutta method once the initial conditions $\alpha(0),\alpha'(0),\xi(0),\xi'(0)$ are given. In this paper, the structural nonlinearities are represented by cubic functions $G(\xi)$ and $M(\alpha)$

$$\begin{aligned} G(\xi) &= \beta_\xi\left(\frac{\varpi}{U}\right)^2\xi^3 \\ M(\alpha) &= \beta_\alpha\left(\frac{1}{U}\right)^2\alpha^3 \end{aligned} \tag{10}$$

where β_ξ and β_α are constants.

3 Averaging Method

As with normal form transformations, the averaging method [10] uses a near identity co-ordinate transformations to simplify a given system of ordinary differential equations. The classical normal form transformation applies to autonomous systems while the averaging method applies to non-autonomous systems. The autonomous differential equations can also be transformed into a non-autonomous system using the method developed by Leung and then analysed using the averaging method outlined here and discussed in detail in [10].

Consider the non-autonomous differential equations

$$X'=\varepsilon h(X,\tau,\varepsilon), \qquad X\in R^p, \qquad |\varepsilon|<<1 \tag{11}$$

where the function $h(X,\tau,\varepsilon)$ is a T-periodic vector field. Using the non-autonomous T-periodic transformation of the form

$$X = \eta + \varepsilon U_1(\eta,\tau) + \varepsilon^2 U_2(\eta,\tau) + \cdots + \varepsilon^k U_k(\eta,\tau) \quad (12)$$

then the resulting averaged equation has terms autonomous up to $O(\varepsilon^k)$ and can be expressed as

$$\eta' = \varepsilon\tilde{h}_1(\eta) + \varepsilon^2\tilde{h}_2(\eta) + \cdots + \varepsilon^k\tilde{h}_k(\eta) + \varepsilon^{k+1}R(\eta,\tau,\varepsilon) \quad (13)$$

The non-autonomous part is truncated and the remaining system of equations is analysed. By using an asymptotic theory, it can be shown that the solution of the final system approximates the solution for the original system (11).

4 Non-linear Analysis

One approach to analyse the stability of non-linear system is to use normal form theory [8]. The non-linear system (8) can be rewritten as

$$X' = \tilde{A}X + G(X,\tau) \quad (14)$$

where $\tilde{A}$ is a constant 8×8 matrix of which all eigenvalues have non-zero real parts. The term $\tilde{A}X$ and $G(X,\tau)$ represent the linear and non-linear parts of the system. This system is further extended to analyse bifurcation behaviour of the aeroelastic system using the system parameter δ defined as

$$\delta = 1 - \frac{\bar{U}_L}{\bar{U}} \quad (15)$$

where $\bar{U}_L$ is constant and equal to the linear flutter speed. By substituting the expression for $\bar{U}$ given in (15) into equation (14), the aeroelastic system of equation (8) can be rewritten as

$$\begin{cases} X' = AX + B(\delta)X + (1-\delta^2)F(X,\tau) \\ \delta' = 0 \end{cases} \quad (16)$$

The matrix A is an 8×8 Jacobian matrix evaluated at the equilibrium point and bifurcation value (i.e. $\delta = 0$). The matrix A has one pair of purely imaginary eigenvalue $\lambda_{1,2} = \pm i\omega$, one pair of complex eigenvalue with negative real part, $\lambda_{3,4} = b \pm ic$, and four negative real eigenvalues $\lambda_5, \lambda_6, \lambda_7, \lambda_8$. The second and third terms in (16) are non-linear functions of δ, X and τ. Expressions for the matrices A and B are given in appendix B. The non-linear part of the system (16) represented by $F(X,\tau)$ is given by

$$F(X) = (0,\ f_2,\ 0,\ f_4,\ 0,\ 0,\ 0,\ 0) \quad (17)$$

where

$$\begin{aligned} f_2 &= j[c_0 M(x_1) - d_0 G(x_3)] - j[c_0 g(\tau) - d_0 f(\tau)] \\ f_4 &= -j[c_1 M(x_1) - d_1 G(x_3)] + j[c_1 g(\tau) - d_1 f(\tau)] \\ j &= 1/(c_1 d_0 - d_1 c_0) \end{aligned} \quad (18)$$

and the coefficients in (18) are given in appendix A.

To apply normal form theory using the averaging method, the system (16) is first transformed into its modal canonical form. A transformation matrix Q is obtained from the eigenspace of A, such that

$$J = Q^{-1}.A.Q = \begin{bmatrix} J_1 & 0 \\ 0 & J_2 \end{bmatrix}, \quad J_1 = \begin{bmatrix} 0 & \omega \\ -\omega & 0 \end{bmatrix},$$
$$J_2 = \begin{bmatrix} b & c & & & & \\ -c & b & & & & \\ & & \lambda_3 & & & \\ & & & \lambda_4 & & \\ & & & & \lambda_5 & \\ & & & & & \lambda_6 \end{bmatrix} \quad (19)$$

Introducing a new variable, Y, such that

$$Y = Q^{-1}.X = (y_1, y_2, \ldots, y_8)^T \quad (20)$$

the system (16) becomes

$$\begin{cases} Y' = J.Y + (Q^{-1}.B(\delta).Q)Y + (1-\delta^2)Q^{-1}.F(Q.Y,\tau) \\ \delta' = 0 \end{cases} \quad (21)$$

The dynamic response of the system (21), which is a 9-dimensional system, can be investigated through a two-dimensional system obtained from the following reduction technique.

5. Liapunov-Schmidt Reduction Technique

The approach based upon the Liapunov-Schmidt reduction technique reduces a multi degree of freedom dynamical system into a two dimensional matrix system corresponding to its critical mode. Thus, higher order normal forms can be obtained for the reduced system.

$$J_3 = \begin{bmatrix} J_1 & 0 \\ 0 & 0 \end{bmatrix}, \quad Z = \begin{bmatrix} y_1 & y_2 & \delta \end{bmatrix}, \qquad W = \begin{bmatrix} y_3 & y_4 & y_5 & y_6 & y_7 & y_8 \end{bmatrix} \tag{22}$$

The system (21) can be split into two systems such that

$$\begin{cases} Z' = J_3.Z + F_Z\left(Z,W\right) \\ W' = J_2.W + F_W\left(Z,W\right) \end{cases} \tag{23}$$

where the first equation in (23) corresponds to the critical mode and F_Z, F_W are non-linear functions of Z and W starting from the second order terms. The first order terms have already been included in the first part associated with Z and W. Since a solution near the origin *Y=(0,0,0,0,0,0,0,0)* is sought, if an approximate function *W = H(Z)* can be found near the origin such that

$$\begin{aligned} W' &= D_Z H(Z)Z' = D_Z H(Z)[J_3 Z + F_Z(Z,H(Z))] \\ &= J_2 H(Z) + F_W(Z,H(Z)) \end{aligned} \tag{24}$$

is valid, then only the first equation in (23) will be needed for the non-linear analysis. In the above relation, the matrix $D_zH(Z)$ is the Jacobian matrix of *H(Z)*. The function *H(Z)* can be approximated by any order function as defined in [11,12]. Here, a second order function is used for which a set of 30 algebraic equation of unknown coefficients were obtained and solved using Mathematica.

6. Test Cases

In order to illustrate the applicability and accuracy of the above approach, two test cases [13] were considered with non-linear terms

$$\begin{aligned} &\bullet \quad (1) \quad \beta_\xi = 0, \quad \beta_\alpha = 3 \\ &\bullet \quad (2) \quad \beta_\xi = 0.1, \quad \beta_\alpha = 40 \end{aligned} \tag{25}$$

In both cases, the analytical predictions were compared with solutions obtained by using the Runge-Kutta numerical time integration for the full system (16). Since the free vibration of the aeroelastic system was sought, the external forces were assumed to be zero, i.e. $P(\tau)=Q(\tau)=0$. The following numerical values are used for the aerofoil geometry and characteristics

$$\begin{aligned} &a_h = 1/2, \quad \mu = 100, \quad x_\alpha = 1/4, \\ &\zeta_\xi = \zeta_\alpha = 0, \quad r_\alpha = 1/2, \quad \varpi = 0.2. \end{aligned} \tag{26}$$

The linear flutter speed of $\overline{U}_L = 0.628509$ and frequency ω_L=0.084 are obtained for $\varpi = 0.2$ using the method developed in [14].

7. Results and Discussion

Applying the above procedure, the system (21) is approximated with a set of two reduced differential equations for each test case:

- Test case 1 with cubic non-linear term in pitch

$$\begin{cases} z_1' = 7.40864\delta z_1 - 3.70432\delta^2 z_1 - 0.013909 z_1^3 + \\ 0.013909\,\delta^2 z_1^3 + 0.125303\,\delta z_2 - 0.0626517\delta^2 z_2 - \\ 0.0018407 z_1^2 z_2 + 0.0018407\delta^2 z_1^2 z_2 - \\ 0.0000811984 z_1 z_2^2 + 0.0000811984\delta^2 z_1 z_2^2 - \\ 1.19397\times 10^{-6} z_2^3 + 1.19397\times 10^{-6}\delta^2 z_2^3 \\ z_2' = 3.13409\delta z_1 - 1.56705\delta^2 z_1 - 0.00536741 z_1^3 + \\ 0.00536741\delta^2 z_1^3 + 0.111982\,\delta z_2 - 0.0559911\delta^2 z_2 - \\ 0.000710316 z_1^2 z_2 + 0.000710316\delta^2 z_1^2 z_2 - \\ 0.000313341 z_1 z_2^2 + 0.000313341\delta^2 z_1 z_2^2 - \\ 4.60746\times 10^{-7} z_2^3 + 4.60746\times 10^{-7}\delta^2 z_2^3 \end{cases} \tag{27}$$

- Test case 2 with cubic non-linear terms in both pitch and heave

$$\begin{cases} z_1' = 7.408648 z_1 - 3.704328^2 z_1 - 0.185086\, z_1^3 + \\ 0.185086\,\delta^2 z_1^3 + 0.125303\,\delta z_2 - 0.0626517\delta^2 z_2 - \\ 0.0242879\, z_1^2 z_2 + 0.0242879\,\delta^2 z_1^2 z_2 - \\ 0.00102374\, z_1 z_2^2 + 0.00102374\,\delta^2 z_1 z_2^2 - \\ 0.0000113788 z_2^3 + 0.0000113788\,\delta^2 z_2^3 \\ z_2' = 3.134098 z_1 - 1.567058^2 z_1 - 0.0715175 z_1^3 + \\ 0.0715175\delta^2 z_1^3 + 0.111982\,\delta z_2 - 0.0559911\delta^2 z_2 - \\ \quad 0.00943767 z_1^2 z_2 + 0.00943767\delta^2 z_1^2 z_2 - \\ \quad 0.000410109\, z_1 z_2^2 + 0.000410109\delta^2 z_1 z_2^2 - \\ \quad 5.5513\times10^{-6} z_2^3 + 5.5513\times10^{-6}\delta^2 z_2^3 \end{cases} \tag{28}$$

Having applied the averaging method for computation of the normal forms up to third order terms, the following normal form solution in the polar co-ordinate system is obtained as

- Test case 1

$$\begin{Bmatrix} r' \\ \theta' \end{Bmatrix} = \begin{Bmatrix} -0.005315\, r^3 + 3.760311\, r\delta - 1.88016\, r\delta^2 + \\ 0.005315\, r^2\delta^2 \\ -0.00178616\, r^2 + 1.50439\,\delta - 0.75219915\delta^2 + \\ 0.00178616\, r^2\delta^2 \end{Bmatrix} \tag{29}$$

- Test case 2

$$\begin{Bmatrix} r' \\ \theta' \end{Bmatrix} = \begin{Bmatrix} -0.070717\, r^3 + 3.760311\, r\delta - 1.88016\, r\delta^2 + \\ 0.070717\, r^2\delta^2 \\ -0.02383\, r^2 + 1.5043935\delta - 0.75219915\delta^2 + \\ 0.0238301\, r^2\delta^2 \end{Bmatrix} \tag{30}$$

The steady state solution for the amplitude of the limit cycles in the transformed domain can be obtained by letting the limit cycle amplitude velocity in equation (29) and (30) be zero. This leads to the expressions

- Test case 1

$$r(\delta) = \frac{\sqrt{\delta(-3.760311 + 1.880156\,\delta)}}{\sqrt{(-0.00531499 + 0.00531499\,\delta^2)}} \tag{31}$$

- Test case 2

$$r(\delta) = \frac{\sqrt{\delta(-3.760311 + 1.880156\,\delta)}}{\sqrt{(-0.070717 + 0.070717\,\delta^2)}} \tag{32}$$

which is a general function based upon the bifurcation parameter δ. The frequency of the limit cycles is also determined as

- Test case 1

$$\omega_{LCO} = \omega_L \begin{pmatrix} 1 - (-0.0017862\, r^2 + 1.5043935\delta - \\ 0.75219915\delta^2 + 0.0017862\, r^2\delta^2) \end{pmatrix} \tag{33}$$

- Test case 2

$$\omega_{LCO} = \omega_L \begin{pmatrix} 1 - (-0.02383\, r^2 + 1.5043935\delta - \\ 0.75219915\delta^2 + 0.0238301\, r^2\delta^2) \end{pmatrix} \tag{34}$$

where r in (33) and (34) is substituted from (31) and (32), respectively. $\omega_L=0.084$ is the linear flutter frequency. The amplitude and frequency of limit cycles are shown in the figure (2) and (3), respectively, for the cases 1 and 2. The time response and the shape of limit cycles at δ=0.06 are illustrated in figure (4) and (5), respectively, for the cases 1 and 2. A near perfect match between analytical and numerical results is obtained for both cases.

Note that the expression for the LCO amplitude and frequency is obtained directly from the analysis, unlike previous work [13] where several approximations have to be used in order to obtain the amplitude-frequency relationship.

8. Conclusions

A non-linear aeroelastic system in functional differential form has been investigated for computation of limit cycle oscillations. The normal form computations were carried out for a general non-autonomous system using the averaging method. This is advantageous compared with other classical methods such as centre manifold theory [13] which only consider autonomous systems.

Since this class of averaging method is best employed for single degree of freedom (SDOF) systems, an approach based upon Liapunov-Schmidt method is used to reduce any large system into its critical SDOF blocks.

The approach is able to predict the amplitude and frequency of LCO for systems with continuous non-linearities. Good agreement was found between the analytical predictions and results from numerical integration.

Research is continuing with the application of the methodology to higher order systems and systems containing non-linear aerodynamics and discontinuous non-linearities.

9. References

[1] AGARD CP566'Advanced Aeroservoelastic Testing and Data Analysis' 1995.

[2] S.J. Price, H. Alighanbari & B.H.K. Lee, 'The Aeroelastic Response of a 2 Dimensional Aerofoil with Bilinear and Cubic Structural Non-*Linearities' J Fluid and Structures v9 1995 pp 175-193*.

[3] G. Dimitriadis & J.E. Cooper, 'Limit Cycle Oscillation Control and Suppression' *Aero Journal v103 1999 pp 257-263*.

[4] L Ruiz-Calavera et al,' A New Compendium of Unsteady Aerodynamic Test Cases for CFD' *Int. Forum on Aeroelasticity and Structural Dynamics 1999 pp 1-12.*

[5] AGARD CP 507'Transonic Unsteady Aerodynamics and Aeroelasticity' 1992.

[6] AGARD Report 822.'Numerical Unsteady Aerodynamics and Aeroelastic Simulation' 1998.

[7] M.Holden, R Brazier & A. Cal,' Effects of Structural Non- Linearities on a Tailplane Flutter Mode' Int. Forum on Aeroelasticity and Structural Dynamics 1995 paper 60.

[8] A.Y.T. Leung, Q.C. Zhang & Y.S. Chen,' Normal Form Analysis of Hopf Bifurcation Exemplified by Duffing's Equation' Journal of Shock and Vibration v1 1994 pp 233-240.

[9] Y.C. Fung, An Introduction to the Theory of Aeroelasticity, *Wiley, New York, 1995*.

[10] A.Y.T. Leung and Z. Qichang, 'Higher-Order Normal Form and Period Averaging', *Journal of Sound and Vibration, 1998.*

[11] A. Sedaghat, J.E. Cooper, J. R. Wright & A.Y.T. Leung, 'Limit Cycle Oscillation Prediction for Non-Linear Aeroelastic Systems with Oscillatory Aerodynamics' *Proc Royal Aero Soc Aerodynamics Conf April 2000*.

[12] A. Sedaghat, J.E. Cooper, J.R. Wright & A.Y.T. Leung, 'Limit Cycle Oscillation Prediction for Aeroelastic Systems with Continuous Non-Linearities' *AIAA-2000-1397. 41st SDM Conference, April 2000.*

[13] L. Liu, Y.S. Wong & B.H.K. Lee, 'Application of the Centre Manifold Theory in Non Linear *Aeroelasticity' Int. Forum on Aeroelasticity and Structural Dynamics 1995 pp 533-542.*

[14] A. Sedaghat, J.E. Cooper, J.R. Wright & A.Y.T. Leung, 'Linear Flutter Prediction using Symbolic *Programming' DYMAC99 1999 pp 37-42.*

10 Acknowledgement

This work was funded by the EPSRC through grant GR/L95175. The authors are also grateful for the support from BAE Systems.

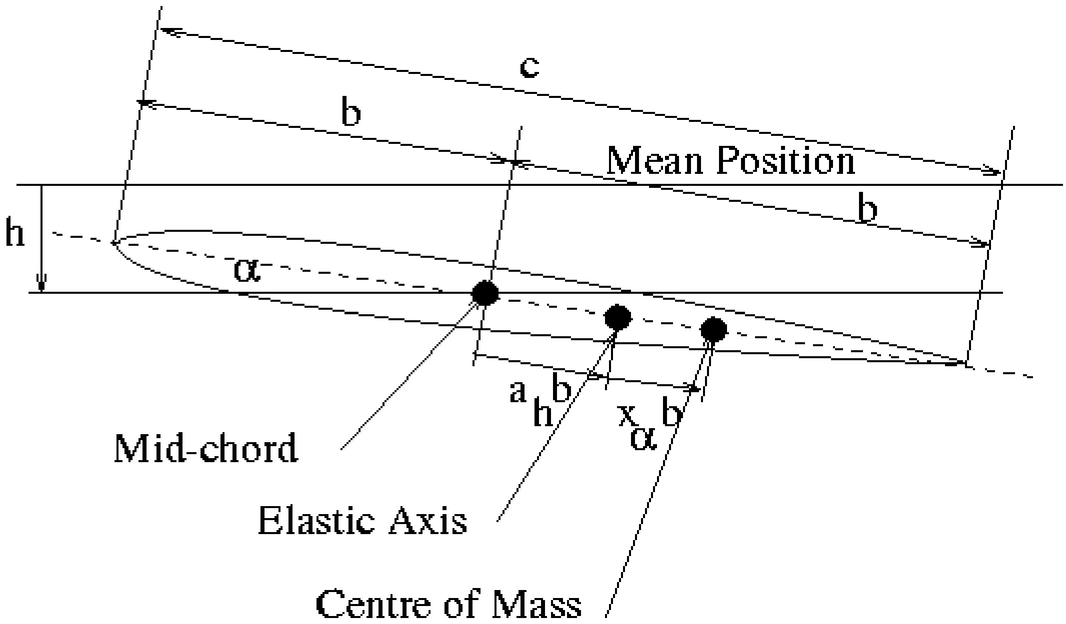

Figure 1. Aerofoil geometry for two degrees of freedom motion.

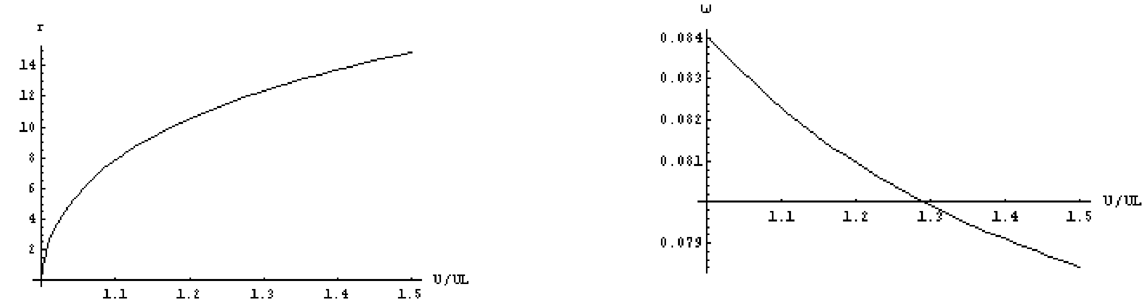

Figure 2. Amplitude and frequency of limit cycle oscillations for test case 1 with cubic nonlinearity in pitch motion.

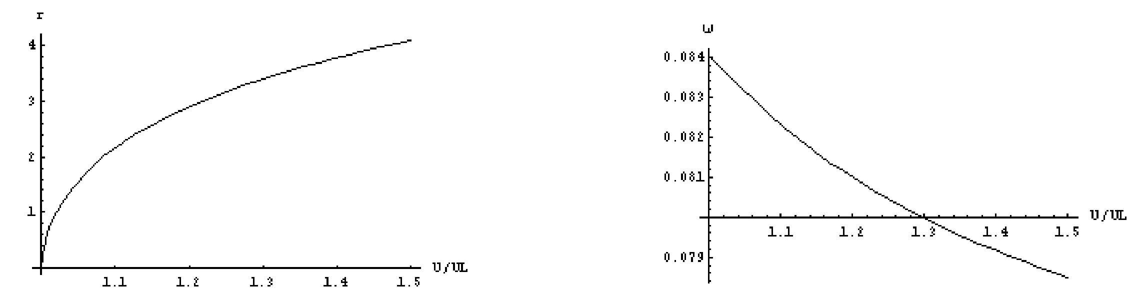

Figure 3. Amplitude and frequency of limit cycle oscillations for test case 2 with cubic nonlinearity in both pitch and heave motion.

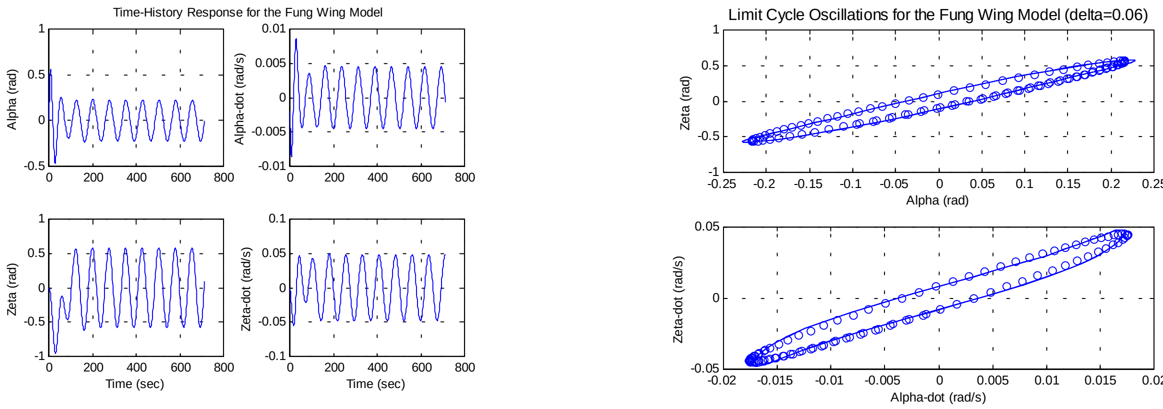

Figure 4. Time response and shape of limit cycle oscillations for test case 1 with cubic nonlinearity in pitch motion at δ=0.06.

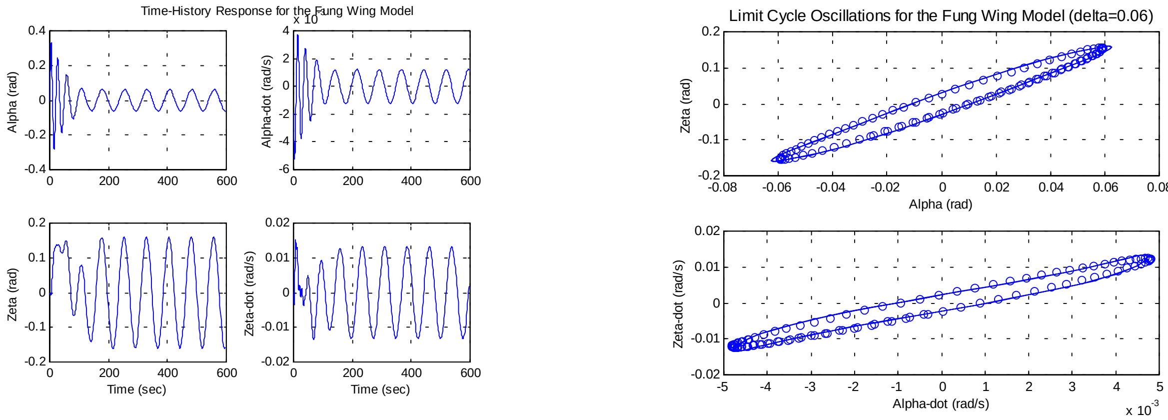

Figure 5. Time response and shape of limit cycle oscillations for test case 2 with cubic nonlinearity in both pitch and heave motion at δ=0.06.

Appendix A

The coefficients of the equation (5) and (8-9) are given as follows

$$c_0 = 1 + \frac{1}{\mu}, \quad c_1 = x_\alpha - \frac{a_h}{\mu}, \quad c_2 = 2\zeta_\xi \frac{\overline{\omega}}{\overline{U}_L} + \frac{2}{\mu}(1-\psi_1-\psi_2), \quad c_3 = \frac{1+2(1/2-a_h)(1-\psi_1-\psi_2)}{\mu},$$

$$c_4 = \frac{2}{\mu}(\psi_1\varepsilon_1 + \psi_2\varepsilon_2), \quad c_5 = \frac{2}{\mu}\left[(1-\psi_1-\psi_2) + (1/2-a_h)(\psi_1\varepsilon_1+\psi_2\varepsilon_2)\right],$$

$$c_6 = \frac{2}{\mu}\psi_1\varepsilon_1\left[1-(1/2-a_h)\varepsilon_1\right], \quad c_7 = \frac{2}{\mu}\psi_2\varepsilon_2\left[1-(1/2-a_h)\varepsilon_2\right], \quad c_8 = -\frac{2}{\mu}\psi_1\varepsilon_1^2, \quad c_9 = -\frac{2}{\mu}\psi_2\varepsilon_2^2,$$

$$d_0 = \frac{x_\alpha}{r_\alpha^2} - \frac{a_h}{\mu r_\alpha^2}, \quad d_1 = 1 + \frac{1+8a_h^2}{8\mu r_\alpha^2}, \quad d_2 = 2\frac{\zeta_\alpha}{U^*} + \frac{1-2a_h}{2\mu r_\alpha^2} - \frac{(1+2a_h)(1-2a_h)(1-\psi_1-\psi_2)}{2\mu r_\alpha^2}$$

$$d_3 = -\frac{(1+2a_h)(1-\psi_1-\psi_2)}{\mu r_\alpha^2} - \frac{(1+2a_h)(1-2a_h)(\psi_1\varepsilon_1+\psi_2\varepsilon_2)}{2\mu r_\alpha^2}, \quad d_4 = -\frac{(1+2a_h)(1-\psi_1-\psi_2)}{\mu r_\alpha^2},$$

$$d_5 = -\frac{(1+2a_h)(\psi_1\varepsilon_1+\psi_2\varepsilon_2)}{2\mu r_\alpha^2}, d_6 = -\frac{(1+2a_h)\psi_1\varepsilon_1\left[1-(1/2-a_h)\varepsilon_1\right]}{\mu r_\alpha^2},$$

$$d_7 = -\frac{(1+2a_h)\psi_2\varepsilon_2\left[1-(1/2-a_h)\varepsilon_2\right]}{\mu r_\alpha^2}, \quad d_8 = \frac{(1+2a_h)\psi_1\varepsilon_1^2}{\mu r_\alpha^2}, \quad d_9 = \frac{(1+2a_h)\psi_2\varepsilon_2^2}{\mu r_\alpha^2}$$

Appendix B

The matrices A and B in the equation (16) are given by

$$A=\begin{bmatrix} A_1 & A_2 \\ A_3 & A_4 \end{bmatrix}, \qquad B=\begin{bmatrix} B_1 & 0 \\ 0 & 0 \end{bmatrix}$$

where

$$A_1=\begin{bmatrix} 0 & 1 & 0 & 0 \\ a_{21} & a_{22} & a_{23} & a_{24} \\ 0 & 0 & 0 & 1 \\ a_{41} & a_{42} & a_{43} & a_{44} \end{bmatrix}, \quad A_2=\begin{bmatrix} 0 & 0 & 0 & 0 \\ a_{25} & a_{26} & a_{27} & a_{28} \\ 0 & 0 & 0 & 0 \\ a_{41} & a_{42} & a_{43} & a_{44} \end{bmatrix}, \quad A_3=\begin{bmatrix} 1 & 0 & 0 & 0 \\ 1 & 0 & 0 & 0 \\ 0 & 0 & 1 & 0 \\ 0 & 0 & 1 & 0 \end{bmatrix},$$

$$A_4=\begin{bmatrix} -\varepsilon_1 & 0 & 0 & 0 \\ 0 & -\varepsilon_2 & 0 & 0 \\ 0 & 0 & -\varepsilon_3 & 0 \\ 0 & 0 & 0 & -\varepsilon_4 \end{bmatrix}, \quad B_1=\begin{bmatrix} 0 & 0 & 0 & 0 \\ b_{21} & b_{22} & b_{23} & b_{24} \\ 0 & 0 & 0 & 0 \\ b_{41} & b_{42} & b_{43} & b_{44} \end{bmatrix}$$

The coefficients $a_{i,j}, b_{i,j}$ are defined as follows

$$\begin{aligned}
&a_{21}=j(d_3c_0-c_5d_0), \quad a_{41}=-j(d_3c_1-c_5d_1),\\
&a_{22}=j(d_2c_0-c_3d_0), \quad a_{42}=-j(d_2c_1-c_3d_1),\\
&a_{23}=j(d_5c_0-c_4d_0), \quad a_{43}=-j(d_5c_1-c_4d_1),\\
&a_{24}=j(d_4c_0-c_2d_0), \quad a_{44}=-j(d_4c_1-c_2d_1),\\
&a_{25}=j(d_6c_0-c_6d_0), \quad a_{45}=-j(d_6c_1-c_6d_1),\\
&a_{26}=j(d_7c_0-c_7d_0), \quad a_{46}=-j(d_7c_1-c_7d_1),\\
&a_{27}=j(d_8c_0-c_8d_0), \quad a_{47}=-j(d_8c_1-c_8d_1),\\
&a_{28}=j(d_9c_0-c_9d_0), \quad a_{48}=-j(d_9c_1-c_9d_1),\\
&b_{21}=jd_{30}c_0, \quad b_{22}=jd_{20}c_0, \quad b_{23}=-jc_{40}d_0, \quad b_{24}=-jc_{20}d_0,\\
&b_{41}=-jd_{30}c_1, \quad b_{22}=-jd_{20}c_1, \quad b_{23}=jc_{40}d_1, \quad b_{24}=jc_{20}d_1
\end{aligned}$$

where the coefficients $c_0, d_0, \ldots, c_9, d_9$ are given in appendix A and the coefficients $j, c_{20}, c_{40}, d_{20}, d_{30}$ are defined below.

$$j=\frac{1}{(c_1d_0-d_1c_0)},$$

$$c_{20}=-2\zeta_\xi\frac{\overline{\omega}}{\overline{U}_L}\delta, \quad c_{40}=\delta(\delta-2)\left(\frac{\overline{\omega}}{\overline{U}_L}\right)^2,$$

$$d_{20}=-2\frac{\zeta_\alpha}{\overline{U}_L}\delta, \quad d_{30}=\delta(\delta-2)\left(\frac{1}{\overline{U}_L}\right)^2.$$